GEOLOGICAL NOTE

Climatic Forcing on Channel Profiles in the Eastern Cordillera of the Coroico Region, Bolivia

Fritz Schlunegger,[1,*] *Kevin P. Norton,*[1,†] *and Gerold Zeilinger*[2,‡]

1. Institute of Geological Sciences, University of Bern, CH-3012 Bern, Switzerland; 2. Institute of Earth and Environmental Sciences, University of Potsdam, D-14476 Potsdam, Germany

ABSTRACT

Orographic precipitation has a large impact on channel morphology and rock uplift via a positive feedback to erosion. We show that in the Eastern Cordillera of Bolivia, channel concavities reach their highest values where annual precipitation increases in the downstream direction, exceeding 3000 mm. The steepest channels are upstream of this zone of high concavity, where precipitation rates are <1000 mm yr^{-1}. Channels exhibit graded forms both upstream and downstream of this transient reach. We conclude that the prolonged effect of orographic erosion and related tectonic uplift is the preservation of channels with extreme concavities in the Eastern Cordillera.

Introduction

The search for tectonic and climate controls on landscape development has become an increasingly important research field in Earth sciences (e.g., Whipple 2009). For instance, a close coupling between surface erosion and tectonic uplift has been documented for the European Alps (Vernon et al. 2009; Norton et al. 2010), the Washington Cascades (Reiners et al. 2003), and the Bolivian Andes (Masek et al. 1994; McQuarrie et al. 2008). Additionally, Finnegan et al. (2008) emphasized that fluvial incision and sediment removal contribute to a positive feedback loop in which high rates of erosional unloading are associated with high rates of rock uplift in the eastern Himalaya. Their findings are supported by geomorphic-, thermochronometric-, and metamorphic-grade data. Interestingly, the strong orographic precipitation gradient that is present in the eastern Himalaya (Bookhagen and Burbank 2006) appears to have little influence on the system (Finnegan et al. 2008). Korup and Montgomery (2009) also find evidence for a positive feedback between erosion and rock uplift in this region but emphasize the importance of glacial controls over erosion. These authors show that moraine dams in the upper catchments are capable of reducing stream power and inhibiting the upstream migration of knickzones, effectively pinning the zone of enhanced exhumation further downstream. The implications of both articles (Finnegan et al. 2008; Korup and Montgomery 2009) are that surface processes act to modulate vertical rock uplift rates, leading to a situation in which more gentle, low-flux headwaters are situated adjacent to a steep, high-flux landscape further downstream.

A similar topographic situation exists for the Eastern Cordillera of Bolivia (fig. 1; Masek et al. 1994), despite differences in subduction direction, crustal architecture, and style of deformation. In particular, in the headwaters of the River Beni, broad valleys of the Cordillera Real give way to the steep, highly erosive slopes of the deeply incised Eastern Cordillera. Safran et al. (2005) showed that ^{10}Be-based denudation rates in this region correlate well with channel steepness patterns and suggested a tectonic control. While Masek et al. (1994) called for an orographic precipitation control on the overall shape of the Beni basin, Safran et al. (2005) did

Manuscript received March 9, 2010; accepted August 17, 2010.

* Corresponding author; e-mail: schlunegger@geo.unibe.ch.
† E-mail: norton@geo.unibe.ch.
‡ E-mail: zeilinger@geo.uni-potsdam.de.

[The Journal of Geology, 2011, volume 119, p. 97–107] 0022-1376/2011/11901-0007$15.00. DOI: 10.1086/657407

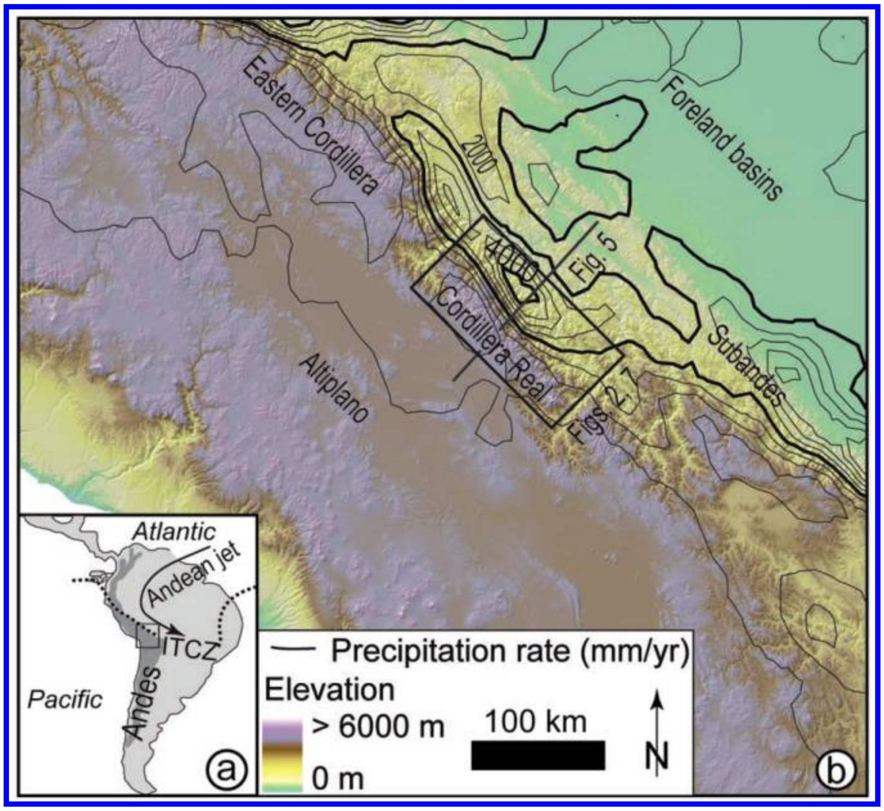

Figure 1. *a*, Overview of the Andean belt and deflection of the Intertropical Convergence Zone (*ITCZ*) during austral summer. *b*, Topography of the Eastern Escarpment with 11-yr mean precipitation contours (TRMM 3B43 V6). The data were acquired using the GES-DISC Interactive Online Visualization and Analysis Infrastructure (Giovanni) as part of NASA's Goddard Earth Sciences (GES) Data and Information Services Center (DISC).

not find explicit correlations between erosion and climate with the existing data sets.

Given that theoretical (e.g., Roe et al. 2002) and large spatial scale (Masek et al. 1994) studies support a climate control, the effects of the well-documented orographic precipitation in Bolivia (Bookhagen and Strecker 2008) should be visible at the reach scale as well. The aim of this article is to explore whether the river basin geometries in the Eastern Cordillera and the uplift pattern can be related to effects of orographic precipitation. To that end, we present a complete morphometric analysis of the upper Beni basin together with new mesoscale (5-km) precipitation data (Bookhagen and Strecker 2008). We focus our study on the central section of the upper Beni basin between the rivers Consata and La Paz (fig. 2). As described by Safran et al. (2005), these two latter basins differ geomorphologically from those of the central section because they have incised into the Altiplano and therefore skew the morphometric data (Zeilinger and Schlunegger 2007). We determine the morphometric characteristics for these rivers (e.g., Tipuani, Challana, Zongo, Coroico, and Tamampaya; fig. 2) from their headwaters to the sub-Andes.

Setting

The Andes of northeastern Bolivia (fig. 1) are a tectonically active mountain belt driven by the subduction of the Brazilian continental shield. This process has controlled the chronology and rates of thrusting and related exhumation on the Altiplano Plateau, the Eastern Cordillera, and the Subandean fold and thrust belt (Gubbels et al. 1993; Allmendinger et al. 1997; Lamb et al. 1997). The Eastern Cordillera experienced a period of intense shortening between the Late Oligocene and the Miocene (Horton and DeCelles 1997; Kley et al. 1997; Gillis et al. 2006) and a phase of accelerated exhumation between the Late Miocene and the present (Gillis et al. 2006). Barke and Lamb (2006) estimated that exhumation was accomplished by rock uplift of ca. 1700 m, with mean erosion of approximately 230

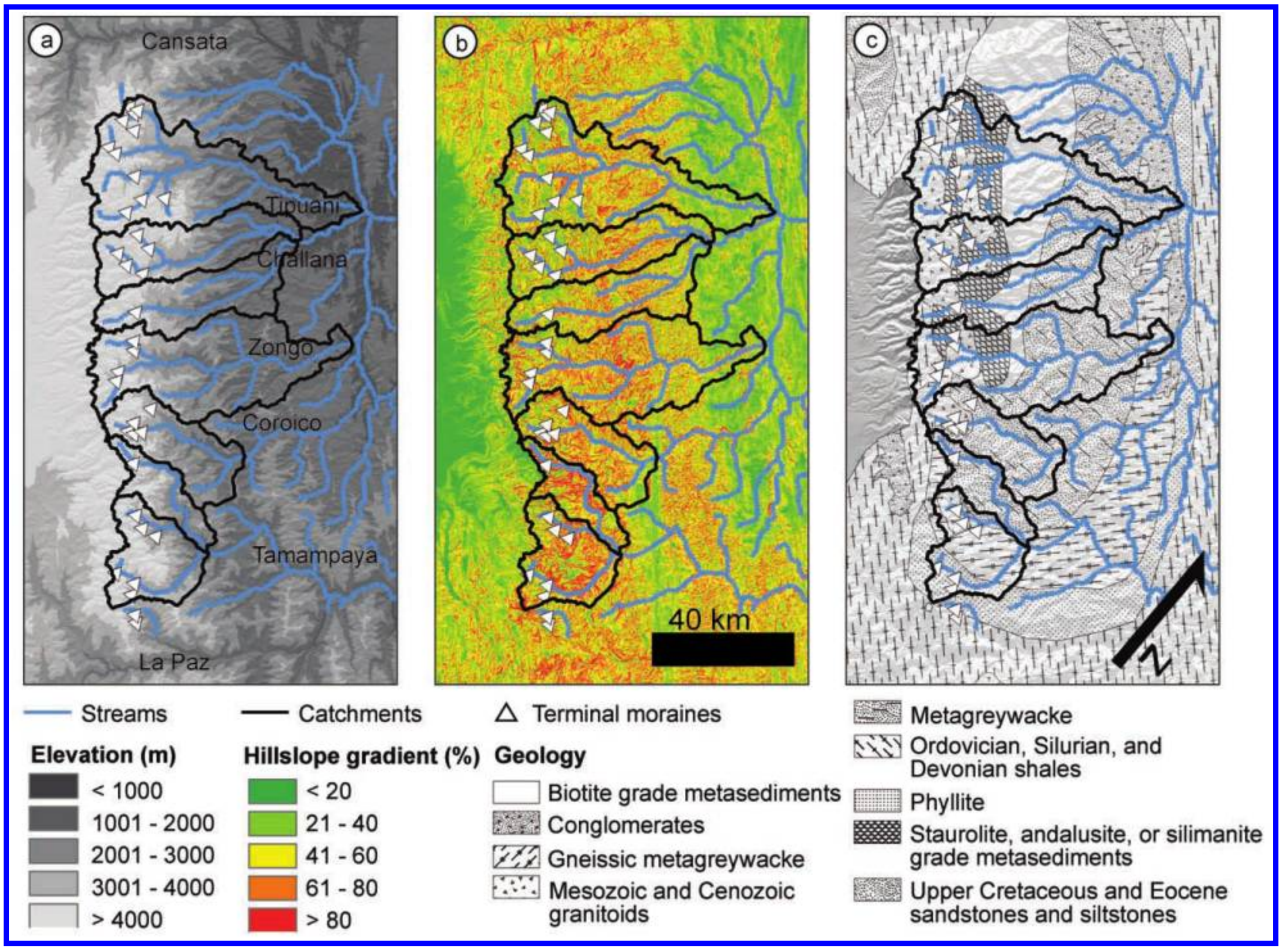

Figure 2. Overview figures showing the morphology of the upper Beni basin. *a*, Elevation and terminal moraines (see also fig. 7*a*), including analyzed streams and watersheds. *b*, Hillslope gradient distribution. *c*, Geological overview map of the eastern segment of the Andes between La Paz and Coroico (modified after Safran et al. 2005).

m particularly in the drier southern Bolivian Andes. The Subandean ranges (fig. 1) form an east-vergent fold and thrust belt made up of Paleozoic, Mesozoic, and Tertiary units (Kley and Monaldi 1998; Echavarria et al. 2003). East of the Subandean ranges, the Rio Beni and Chaco basins rest on the Brazilian Shield and represent the modern foreland basin deposits.

The Eastern Cordillera hosts a network of branched channels that drain the ca. 400–1500-km^2-large tributary basins of the Beni River (fig. 2). These rivers originate in the Cordillera Real, where peak elevations exceed 5000 m asl. The tributary rivers converge along the base of the Eastern Cordillera before cutting across the anticlines of the Subandean fold and thrust belt. Remnants of low-relief, ca. 12–3-million-year-old pediplains (Kennan et al. 1997; Barke and Lamb 2006) are preserved in few locations. Concentrations of cosmogenic nuclides in river-born sand (Safran et al. 2005) and suspended loads of sediments (Bourges et al. 1990; Aalto et al. 2006) yield erosion rates between 0.04 and 1.35 mm/yr on millennial to decadal timescales.

Precipitation in the central Andes is mainly sourced in the Atlantic (fig. 1) with recycled humidity from the Amazon Basin (Salio et al. 2002). Most of this moisture is lost in the Subandean ranges and the Eastern Cordillera. In this latter mountain belt, the orographic barrier results in rainfall in excess of 3500 mm/yr (fig. 1*b*; Bookhagen and Strecker 2008). Maximum rainfall intensity occurs during austral summer, from December to February, when the low-level Andean jet stream and the Intertropical Convergence Zone (fig. 1*a*) are near their southernmost positions (Garreaud et al. 2003). Orbital variations (Garreaud et al. 2003) are recorded by multiple lake-level highstands on the

Altiplano (e.g., Baker et al. 2001*a*, 2001*b*; Fritz et al. 2004, 2007; Placzek et al. 2006). The precipitation cycles related to the expansion of the equatorial easterlies (Garreaud et al. 2003) have been traced back to at least the Middle Miocene (Kaandrop et al. 2005) presumably in response to the rise of the Andes (Strecker et al. 2007; Uba et al. 2007; Ehlers and Poulsen 2009).

Data Sources and Methods

Because moraine dams in upper catchments are considered to be capable of effectively pinning the zone of enhanced exhumation further downstream (e.g., Korup and Montgomery 2009), we mapped the positions of end moraines and potential moraine dams from Landsat ETM+ panchromatic band imagery at a resolution of ~25 m. In cases where the end moraines were no longer visible, the extrapolated locations of lateral moraines were used. The moraine locations were verified against those of Klein and Isacks (1998).

We evaluated large-scale patterns of climate and tectonic forcing on the landscape's morphology using simple relationships between uplift, erosion, and upstream size of the drainage basin. If rock uplift U is compensated by erosion E (e.g., Tucker and Slingerland 1997), then

$$U = E = k_b Q^m S^n, \tag{1}$$

where k_b is related to erosivity, S is the local stream gradient, and Q is water discharge. In this case, the local stream gradient can be calculated as

$$S = \sqrt[n]{\frac{U}{k_b}} Q^{-m/n} = \sqrt[n]{\frac{U}{k_b}} (PA)^{-m/n}, \tag{2}$$

where PA approximates water discharge Q and is the product of precipitation rate P and size of the upstream drainage basin A.

Equation (2) has the same form as Flint's (1974) power law relationship between stream gradient and upstream size of the drainage basin:

$$S = k_s A^{-\theta}, \tag{3}$$

where k_s and θ are referred to as steepness and concavity indices, respectively, and are equal to $k_s = (U/k_b)^{1/n}$and $\theta = m/n$. Accordingly, any variations in rock uplift patterns can be identified by a corresponding change in the channel's steepness, if k_b remains constant and streams display graded longitudinal profiles (Wobus et al. 2006; Ouimet et al. 2009). Similarly, orographic precipitation gradients will correspond with a downstream increase in water discharge near the headwaters, which is directly reflected by the stream's concavity θ (Roe et al. 2002; Zaprowski et al. 2005). As a consequence, the largest climate imprints on channel profiles are expected where the change in downstream precipitation gradients is highest (i.e., where the second derivative of precipitation rate reaches a maximum), reflected by maximum concavities θ_{max} (Roe et al. 2002). Accordingly, for each stream within the study area, we calculated changes in downstream precipitation gradients and extracted concavity indices from log(S)-log(A), plots where

$$\log(S) = k_s - \theta \times \log(A). \tag{4}$$

Steepness values k_s were normalized relative to a reference concavity of 0.45 for comparison, which has become a standard in geomorphology (e.g., Wobus et al. 2006). Slopes are determined from the void-filled Shuttle Radar Topography Mission V4 90-m digital elevation model (Jarvis et al. 2008) provided by the Consultative Group on International Agricultural Research (http://srtm.csi.cgiar.org).

Results

Moraines occur at elevations ranging from ~3000 to 4400 m (fig. 2*a*), with the majority of the mapped moraines being either weakly expressed or significantly eroded. Substantial (i.e., several kilometers long) latero-frontal moraines are found only above ~3500 m. Unlike the situation in the eastern Himalaya (Korup and Montgomery 2009), the moraines in the upper Beni catchment occur both above and beneath the incised reaches and the prominent fluvial knickzones (see also Klein and Isacks 1998).

Plots of log(S)-log(A) of the major streams draining the midsection of the Beni headwaters show three distinct segments (fig. 3*b*–3*h*). The upper reaches of each system are characterized by low channel steepnesses and low channel concavities, which grade into a typically broad rollover zone of negative concavities and increasing steepnesses (e.g., a knickzone). Hillslopes in this upper region average 54% ± 6% (fig. 4). Downstream of this knickzone is a middle section with concavity values of 0.8 to ~4 (fig. 3*b*–3*h*). These values are between two and six times larger compared with mean values from graded steady state rivers in tectonically active mountain belts (e.g., Korup 2006). Channels in this middle section reach steepness values up to 600 $m^{0.9}$ (fig. 5*b*) and are bordered by hillslopes with mean gradients of 60% ± 6% (figs. 4, 5*d*), hosting abundant landslides (Blodgett et al.

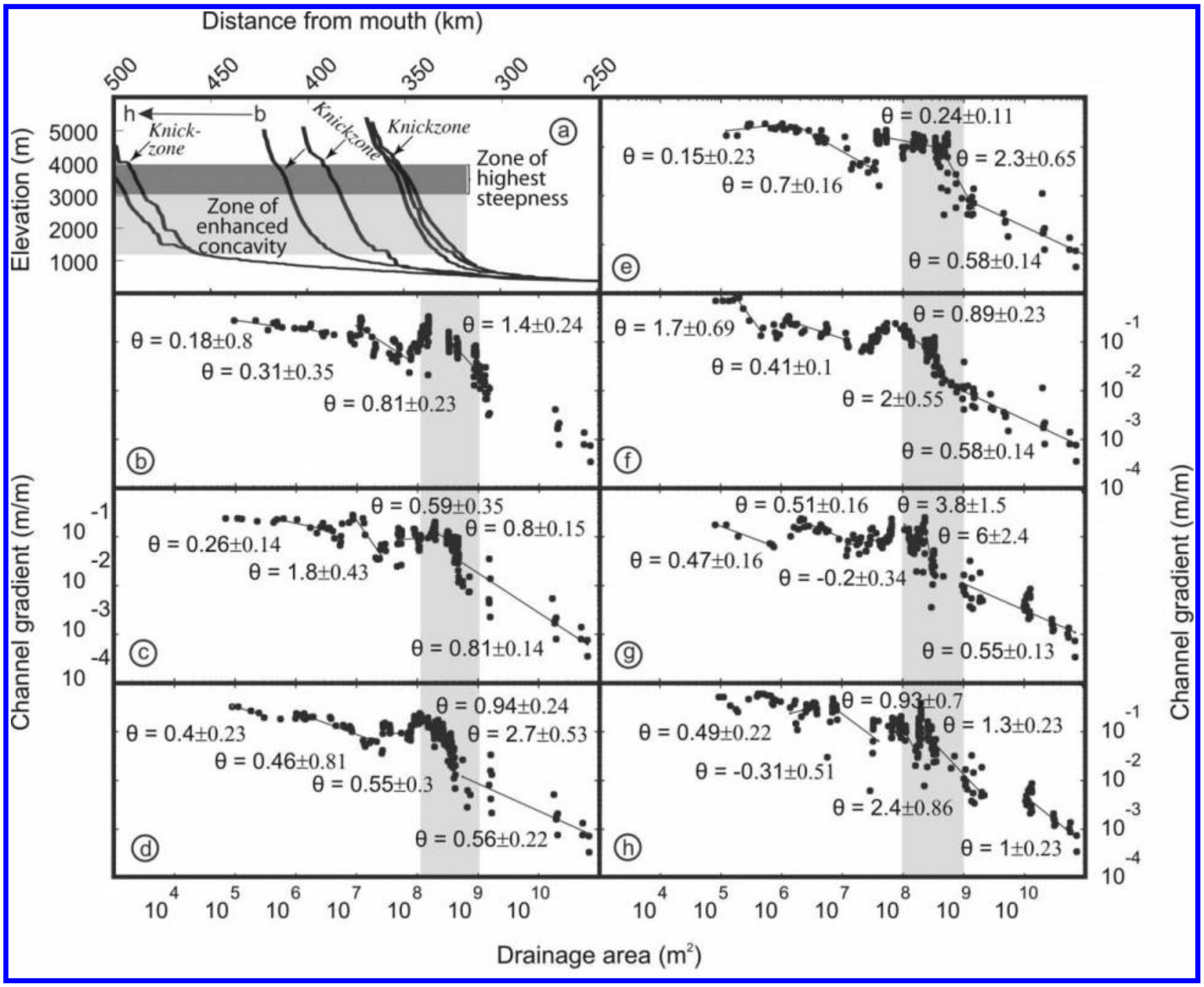

Figure 3. Stream profiles and slope-area relationships for the study catchments. *a*, Longitudinal stream profiles for each stream showing the zone of enhanced concavity and high steepness (*gray shading*) determined from the slope-area plots for each stream (*b–h*).

2007). Finally, near the Subandean range, channel steepness indices and concavities return to nearly the identical low values as in the upper reaches, and hillslope gradients average 48% ± 8% (e.g., fig. 2*b*). Interestingly, maximum steepness values are found at elevations of ~2800–4000 m asl, while high concavity values occur further downstream at elevations between ~1200 and 3000 m asl (fig. 3*a*) and coincide spatially with the segment where downstream precipitation gradients are high (fig. 5). The peak concavity values occur in a limited reach of ca. 15 km length that experiences the most rapid downstream increase in precipitation rates (figs. 5, 6). Our results also support the findings of Safran et al. (2005) that channel steepness indices do not depend systematically on underlying lithology (e.g., fig. 2*c*).

Discussion

Because the Bolivian Andes express a topographic form similar to the eastern Himalaya (Masek et al. 1994), it is possible that these landscapes—with low-gradient upper reaches followed by a steep, incised zone—also result from a similar genesis, despite differences in crustal properties and subduction direction. The nature of the moraines in the upper catchments of the Beni River makes it unlikely that they are responsible for maintaining this landscape. In particular, the moraines are in some

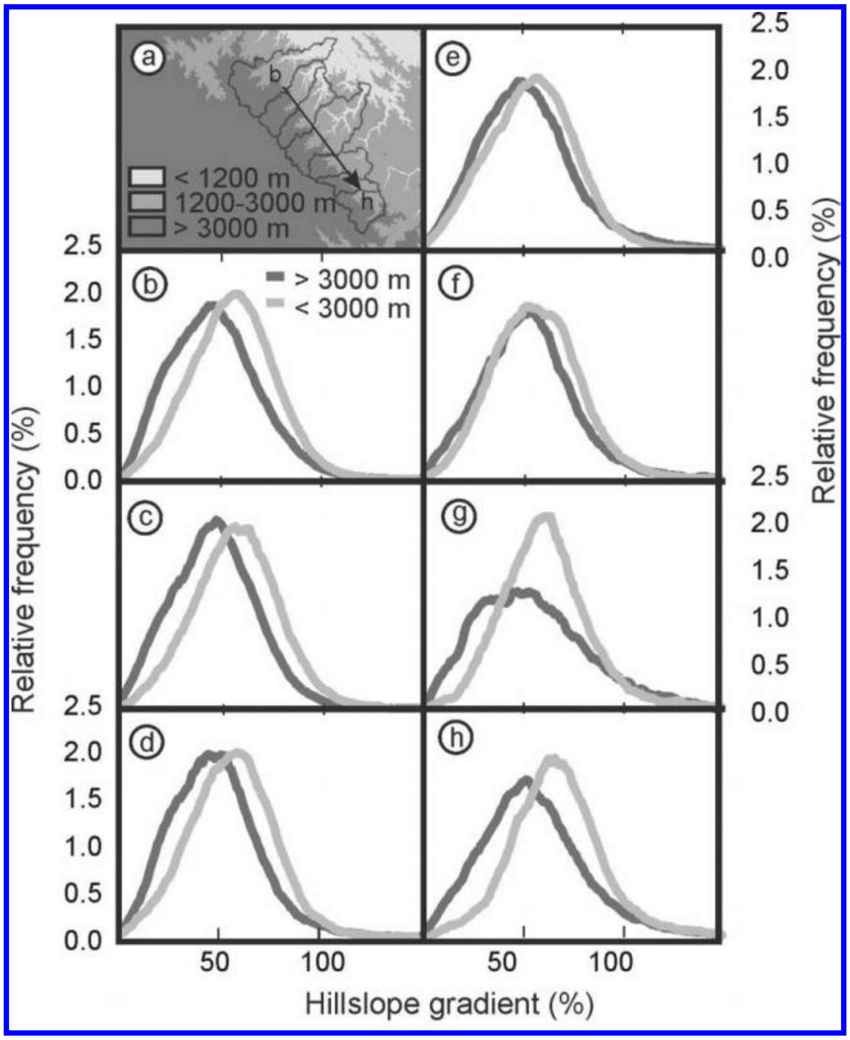

Figure 4. Hillslope gradient distributions above 3000 m and in the elevation range from 1200 to 3000 m (i.e., the enhanced concavity zone) for the studied catchments (*b*–*h*). The average gradients are skewed to higher values within the zone of high concavity (see fig. 3).

cases situated within the zones of high channel steepness, suggesting that they are not retarding channel incision (fig. 7*a*). We also note that moraines are very weakly expressed below ~3500 m (see also Klein and Isacks 1998), either because the glaciers themselves were not highly erosive, or because the moraines were rapidly eroded. In either case, the moraines in the upper Beni basin are not capable of creating significant dams in contrast to those in the Himalaya (Korup and Montgomery 2009).

The potential tectonic control reported by Finnegan et al. (2008) for the eastern Himalaya has also been suggested for the Eastern Cordillera and the upper Beni region (Safran et al. 2005). However, in both cases (Safran et al. 2005; Finnegan et al. 2008) it was not possible to show a correspondence between topographic properties and climate. We suggest that this is due to a mismatch between the scales of topographic processes and the scales of available precipitation data. Here, we are able to use a new database of precipitation rates that corresponds to the hillslope-scale geomorphic processes (Bookhagen and Strecker 2008). As has been suggested from the continental scale (Zaprowski et al. 2005), there should be a correlation between high precipitation rates and high channel concavities. Roe et al. (2002) explored the theoretical relationships and showed that for graded streams, concavities >1 occur only where precipitation rates increase in the downstream direction. We extend this view in figure 5*e*, which additionally shows

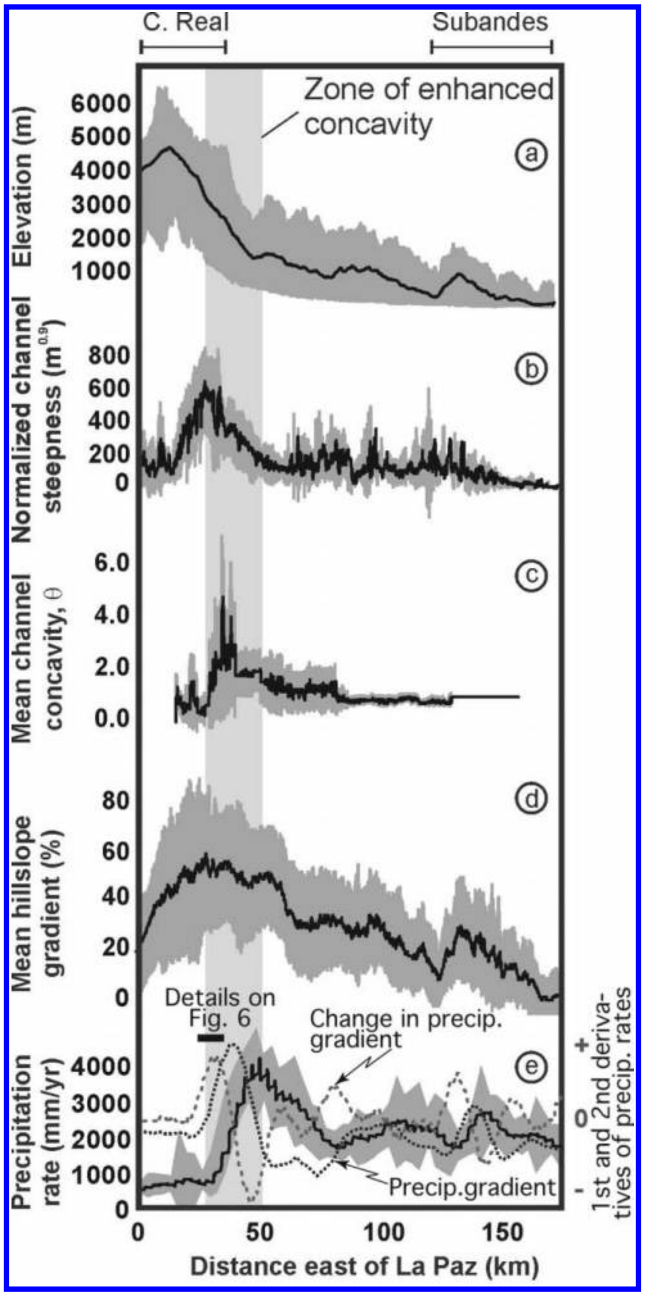

Figure 5. Profiles along an N45E line from La Paz to the Subandes. *a*, Minimum and maximum elevations (*gray shading*) and mean (*solid line*). In *b–e*, the gray shading shows 1 SD from the mean. *b*, Channel steepness normalized to a reference concavity of 0.45 (Wobus et al. 2006). *c*, Channel concavity of the major streams determined from slope-area relationships (see fig. 3*b*–3*h*). Note that *c* is shorter than *b* because it is necessarily calculated over a longer-reach scale than the normalized steepness (Wobus et al. 2006). *d*, Mean hillslope gradient (*solid line*). *e*, Annual precipitation rate (TRMM 2B31 data; *solid line*; Bookhagen and Strecker 2008, swath 74). The downstream precipitation gradient corresponds to the first derivative, and the change in downstream precipitation gradient corresponds to the second derivative of precipitation. Further correlation details are presented in figure 6.

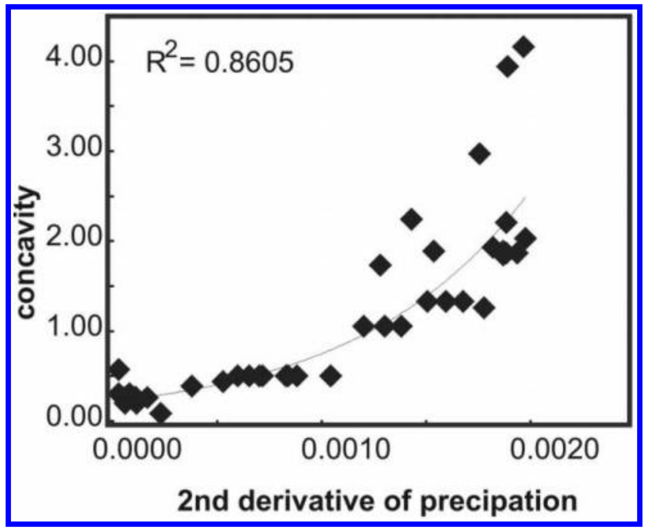

Figure 6. Relationship between change in downstream precipitation gradient (second derivative of precipitation) and concavity values measured over the zone of initial precipitation increase (25–40 km downstream; fig. 5*e*).

that high concavities occur where downstream precipitation gradients (first derivative) are high. In addition, concavities reach maximum values with the most rapid downstream increase (second derivative; figs. 5*d*, 6). We see this effect most clearly near the headwaters because inferred discharge is lowest and the absolute change in precipitation rates is highest for these reaches. Accordingly, downstream increasing precipitation gradients have the largest impact on water discharge in the headwaters, as seen in the corresponding increase in concavity values. Potential similar effects further downstream are damped because any variations in precipitation will not have a large effect on the already high cumulative discharge. In addition, a segment with high steepness values is created at the upper end of the zone of high concavity. This leads to the formation of a knickzone, where a slowly eroding plateau with smooth hillslopes is juxtaposed to a rapidly eroding reach with elevated channel steepness, high erosion rates, and steep hillslopes (Safran et al. 2005; Blodgett and Isacks 2007).

In the absence of any perturbing force, the longterm evolution of a knickzone is the reduction of peak and ridge heights and a return to graded lon-

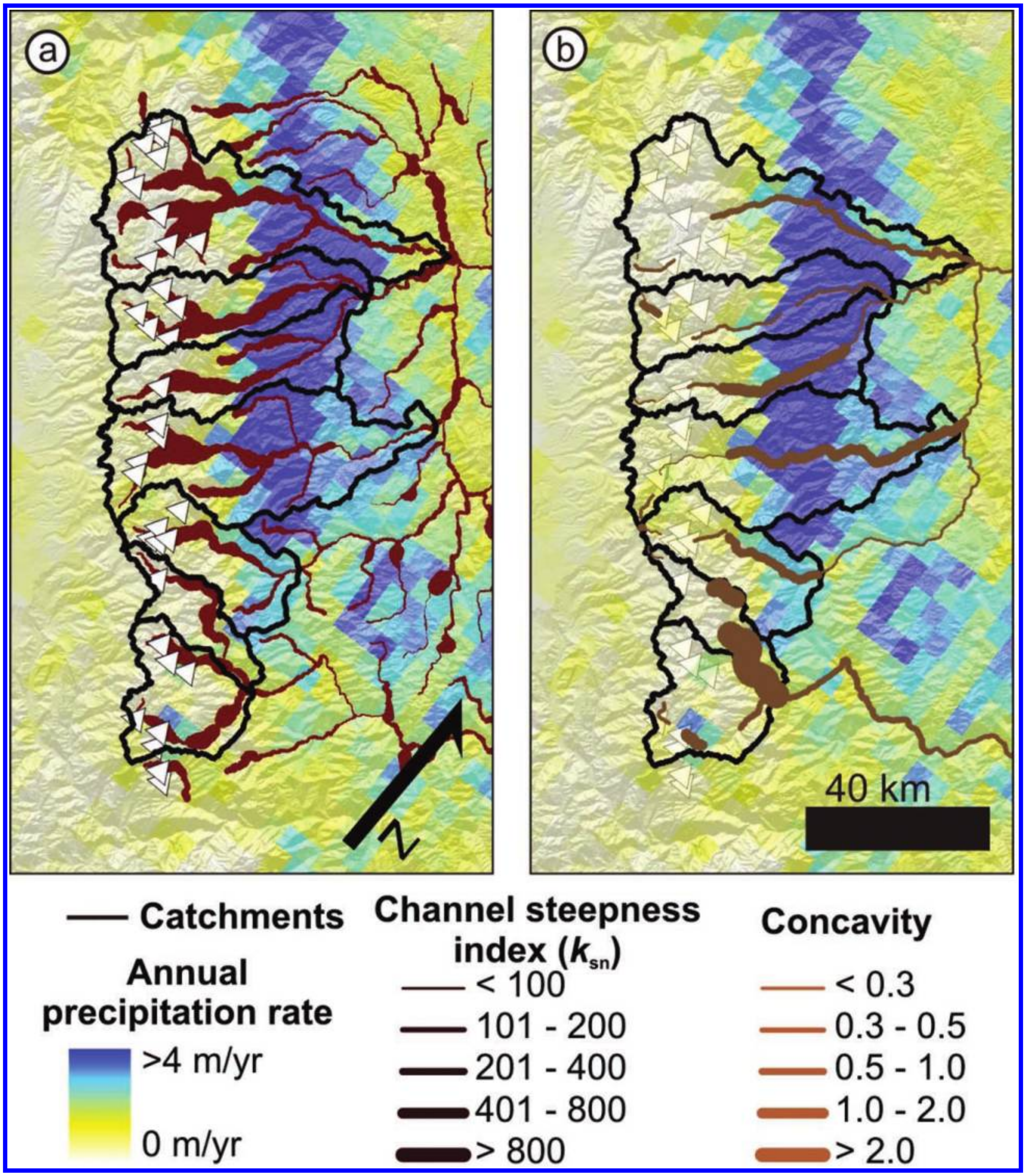

Figure 7. Relationship of normalized channel steepness (*a*; see also Safran et al. 2005) and channel concavity (*b*) to TRMM-derived annual precipitation rates (Bookhagen and Strecker 2008) and the location of potential moraine dams.

gitudinal stream profiles and lowered stream concavities (Whipple 2004; Zaprowski et al. 2005; fig. 8*a*). In the Eastern Cordillera, the pattern of erosion, however, is most likely long lived as the short-term (cosmogenic nuclide) erosion rates are within the range of long-term (thermochronometry) rates, suggesting that there has been no significant change in exhumation rates in the past few million

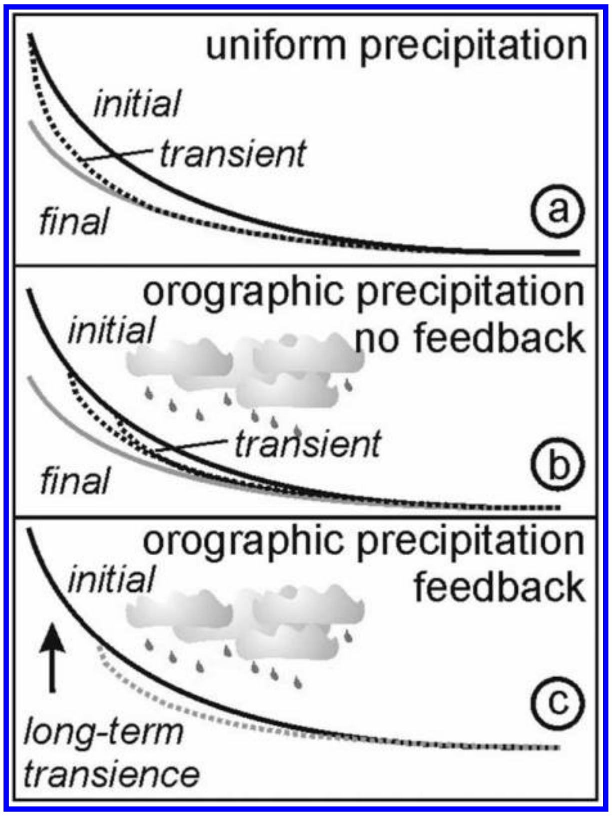

Figure 8. Conceptual model for the maintenance of irregular channel profiles in response to orographic precipitation. *a*, In the case of a uniform increase in precipitation rates, an initial phase of increased concavity is followed by lowering of the headwaters and a return to lower concavities (e.g., Zaprowski et al. 2005). *b*, In the presence of orographic precipitation, the zone of increased concavity results in a transient reach. *c*, Tectonic response to incision maintains the height of the headwaters by a positive tectonic feedback to focused erosion, thereby preserving the orographic precipitation gradient and the resulting steep and highly concave transient channel reaches during headward retreat.

years (Safran et al. 2005, 2006; Wittmann et al. 2009). Additionally, the rise of the Altiplano to elevations where the Andean topography interferes with the rainfall and exhumation pattern is thought to have occurred no later than the late Miocene (Gubbels et al. 1993; Kaandrop et al. 2005; Barke and Lamb 2006; McQuarrie et al. 2008; Barnes and Ehlers 2009). These arguments suggest that the modern precipitation and erosion patterns are likely to have existed for several millions of years. Accordingly, the juxtaposition of a slowly eroding plateau and a rapidly eroding knickzone requires a mechanism that is capable of maintaining the gentle high elevations of the headwaters and a transient longitudinal stream profile with a distinct knickzone (fig. 7) over timescales of millions of years.

On the basis of a coupled erosional-flexural one-dimensional model, Masek et al. (1994) showed that the maintenance of high elevations in the headwaters can be explained by a positive tectonic feedback to orographic-driven erosion. In this case, fast erosion rates lead to rock uplift via flexural isostatic compensation. In the upper Beni basin, the reaches with maximum steepness and concavity values result in erosional unloading over a ca. 20-km-long spatial scale (Safran et al. 2005; Blodgett and Isacks 2007). The effect of this focused erosion on rock uplift then critically depends on the mechanical properties of the underlying crust and particularly on the flexural rigidity or elastic thickness of the plates involved. Estimates for elastic thicknesses range from 30 to 40 km, with extreme values as low as 15 km (Tassara et al. 2007) and as high as 50 and 75 km (Watts et al. 1995). These elastic thicknesses correspond to flexural rigidity values between 10^{22} and 10^{24} Nm. Montgomery and Stolar (2006) showed that the wavelength of response for flexural rigidities greater than ~10^{21} Nm are independent of the size of the incising valley and greater than 100 km. Indeed, for a flexural rigidity greater than the minimum of 10^{22} Nm, the wavelength of response to focused erosion would be as wide as the entire upper Beni basin. Hence, headwater elevations can be maintained (or indeed rise; Barnes and Ehlers 2009) over millions of years, because the scale of tectonic accommodation to focused erosional unloading encompass the entire drainage basin, including the headwaters. The nearly identical steepness and concavity values above and beneath the segments of incision (figs. 3*b*–3*h*, 5*b*, 5*c*) support this interpretation, requiring a long-wavelength forcing. In this case, the combination of focused erosion and a longer-wavelength positive tectonic feedback results in the preservation of highly elevated headwaters. This is a prerequisite for the maintenance of the orographic precipitation pattern and the resulting highly concave transient sections during headward retreat. Indeed, if the relief were not maintained, then precipitation would travel further upstream, causing rapid erosion of the plateau, as is the case for the adjacent La Paz and Consata basins north and south of the study transect.

ACKNOWLEDGMENTS

Research was funded through the Swiss National Science Foundation project 20021 awarded to F.

Schlunegger. We would like to thank B. Bookhagen for providing the precipitation data. The constructive reviews by E. Safran and an anonymous reviewer are greatly acknowledged.

REFERENCES CITED

Aalto, R.; Dunne, T.; and Guyot, J. L. 2006. Geomorphic controls on Andean denudation rates. J. Geol. 114:85–99.

Allmendinger, R. W.; Jordan, T. E.; Kay, S. M.; and Isacks, B. L. 1997. The evolution of the Altiplano-Puna Plateau of the central Andes. Annu. Rev. Earth Planet. Sci. 25:139–174.

Baker, P. A.; Seltzer, G. O.; Fritz, S. C.; Dunbar, R. B.; Grove, M. J.; Cross, S. L.; Tapia, P.; Rowe, H. D.; and Broda, J. P. 2001*a*. The history of South American tropical precipitation for the past 25,000 years. Science 291:640–643.

———. 2001*b*. Tropical climate changes at millennial and orbital timescales on the Bolivian Altiplano. Nature 409:698–701.

Barke, R., and Lamb, S. 2006. Late Cenozoic uplift of the Eastern Cordillera, Bolivian Andes. Earth Planet. Sci. Lett. 249:350–367.

Barnes, J. B., and Ehlers, T. A. 2009. End member models for Andean Plateau uplift. Earth-Sci. Rev. 97:105–132.

Blodgett, T. A., and Isacks, B. L. 2007. Landslide erosion rate in the Eastern Cordillera of northern Bolivia. Earth Interact. 11:1–30.

Bookhagen, B., and Burbank, D. W. 2006. Topography, Relief, and TRMM-derived rainfall variations along the Himalaya. Geophys. Res. Lett. 33:L08405, doi:10:1029/2006GL026037.

Bookhagen, B., and Strecker, M. 2008. Orographic barriers, high-resolution TRMM rainfall, and relief variations along the eastern Andes. Geophys. Res. Lett. 35:L06403, doi:10.1029/2007GL032011.

Bourges, J.; Guyot, J. L.; Carrasco, M.; Barragan, M. C.; and Cortes, J. 1990. Évolution spatio-temporelle des debits de des matières particulaires sur un basin des Andes boliviennes: le Rio Béni. IAHS Publ. 193:351–356.

Echavarria, L.; Hernandez, R.; Allmendinger, R.; and Reynolds, J. 2003. Subandean thrust and fold belt of northwestern Argentina: geometry and timing of the Andean evolution. Am. Assoc. Pet. Geol. Bull. 87:965–985.

Ehlers, T. A., and Poulsen, C. J. 2009. Influence of Andean uplift on climate and paleoaltimetry estimates. Earth Planet. Sci. Lett. 281:238–248.

Finnegan, N. J.; Hallet, B.; Montgomery, D. R.; Zeitler, P. K.; Stone, J. O.; Anders, A. M.; and Yuping, L. 2008. Coupling of rock uplift and river incision in the Namche Barwa–Gyala Peri massif, Tibet. Geol. Soc. Am. Bull. 120:142–155.

Flint, J. J. 1974. Stream gradient as a function of order, magnitude, and discharge. Water Resour. Res. 10:969–973.

Fritz, S. C.; Baker, P. A.; Lowenstein, T. K.; Seltzer, G. O.; Rigsby, C. A.; Dwyer, G. S.; Tapia, P. M.; Arnold, K. K.; Ku, T. L.; and Luo, S. 2004. Hydrologic variation during the last 170,000 years in the Southern Hemisphere tropics of South America. Quat. Res. 61:95–104.

Fritz, S. C.; Baker, P. A.; Seltzer, G. O.; Ballantyne, A.; Tapia, P.; Cheng, H.; and Edwards, R. L. 2007. Quaternary glaciation and hydrologic variation in the South American tropics as reconstructed from the Lake Titicaca drilling project. Quat. Res. 68:410–420.

Garreaud, R.; Vuille, M.; and Clement, A. C. 2003. The climate of the Altiplano: observed current conditions and mechanisms of past changes. Paleogeogr. Paleoclimatol. Paleoecol. 194:5–22.

Gillis, R. J.; Horton, B. K.; and Grove, M. 2006. Thermochronology, geochronology and upper crustal structure of the Cordillera Real: implications for Cenozoic exhumation history of the central Andean Plateau. Tectonics 25:TC6007, doi:10.1029/2005TC001887.

Gubbels, T. L.; Isacks, B. L.; and Farrar, E. 1993. High-level surfaces, plateau uplift, and foreland development, Bolivian central Andes. Geology 21:695–698.

Horton, B. K., and DeCelles, P. G. 1997. The modern foreland basin system adjacent to the central Andes. Geology 25:895–898.

Jarvis, A.; Reuter, H. I.; Nelson, A.; and Guevara, E. 2008. Hole-filled SRTM for the globe. Version 4. http://srtm.csi.cgiar.org.

Kaandrop, R. J. G.; Vonhof, H. B.; Wesselingh, F. P.; Pittman, L. R.; Kroon, D.; and van Hinte, J. E. 2005. Seasonal Amazonian rainfall variation in the Miocene climate optimum. Paleogeogr. Paleoclimatol. Paleoecol. 221:1–6, doi:10.1016/j.palaeo.2004.12.024.

Kennan, L.; Lamb, S.; and Hoke, L. 1997. High-altitude paleosurfaces in the Bolivian Andes: evidence for late Cenozoic surface uplift. *In* Widdowson, M., ed. Paleosurfaces: recognition, reconstruction and paleoenvironmental interpretation. Geol. Soc. Lond. Spec. Publ. 120:307–323.

Klein, A. G., and Isacks, B. L. 1998. Alpine glacial geomorphological studies in the central Andes using Landsat Thematic Mapper images. Glacial Geol. Geomorphol. http://ggg.qub.ac.uk/papers/full/1998/rp011998/rp01.pdf.

Kley, J., and Monaldi, C. R. 1998. Tectonic shortening and crustal thickening in the central Andes: how good is the correlation? Geology 26:723–726.

Kley, J.; Müller, J.; Tawackoli, S.; Jacobshagen, V.; and Manutsoglu, E. 1997. Pre-Andean and Andean-age deformation in the Eastern Cordillera of southern Bolivia. J. S. Am. Earth Sci. 10:1–19.

Korup, O. 2006. Rock-slope failure and the river long profile. Geology 34:45–48.

Korup, O., and Montgomery, D. 2009. Tibetan Plateau river incision inhibited by glacial stabilization of the

Tsangpo Gorge. Nature 455:786–790, doi:10.1038/nature07322.

Lamb, S. H.; Hoke, L.; Kennan, L; and Dewey, J. 1997. Cenozoic evolution of the central Andes in Bolivia and northern Chile. *In* Burg, J. P., and Ford, M., eds. Orogeny through time. Geol. Soc. Lond. Spec. Publ. 121: 337–264.

Masek, J. G.; Isacks, B. L.; and Fielding, E. J. 1994. Erosion and tectonics at the margins of continental plateaus. J. Geophys. Res. 99:13941–13956.

McQuarrie, N.; Ehlers, T. A.; Barnes, J. B.; and Meade, B. 2008. Temporal variation in climate and tectonic coupling in the central Andes. Geology 36:999–1002, doi:10.1130/G25124A.1.

Montgomery, D. R., and Stolar, D. B. 2006. Reconsidering Himalayan river anticlines. Geomorphology 82:4–15.

Norton, K. P.; Abbühl, L. M.; and Schlunegger, F. 2010. Glacial conditioning as an erosional driving force in the Central Alps. Geology 38:655–658.

Ouimet, W. B.; Whipple, K. X.; and Granger, D. E. 2009. Beyond threshold hillslopes: channel adjustment to base-level fall in tectonically active mountain ranges. Geology 37:579–582.

Placzek, C.; Quade, J.; and Patchett, P. J. 2006. Geochronology and stratigraphy of late Pleistocene lake cycles on the southern Bolivian Altiplano: implication for causes of tropical climate change. Geol. Soc. Am. Bull. 118:515–532.

Reiners, P. W.; Ehlers, T. A.; Mitchell, S. G.; and Montgomery, D. R. 2003. Coupled spatial variations in precipitation and long-term erosion rates across the Washington Cascades. Nature 426:645–647, doi:10.1038/nature02111.

Roe, G. H.; Montgomery, D. R.; and Hallet, B. 2002. Effects of orographic precipitation variations on the concavity of steady-state river profiles. Geology 30:143–146.

Safran, E. B.; Biermann, P. R.; Aalto, R.; Dunne, T.; Whipple, K. X.; and Caffee, M. 2005. Erosion rates driven by channel network incision in the Bolivian Andes. Earth Surface Process. Landforms 30:1007–1024, doi:10.1002/esp.1250.

Safran, E. B.; Blythe, A.; and Dunne, T. 2006. Spatially variable exhumation rates in orogenic belts: an Andean example. J. Geol. 114:665–681.

Salio, P.; Nicolini, M; and Saulo, A. C. 2002. Chaco low-level jet events characterization during the austral summer season. J. Geophys. Res. 107:4816, doi:10.1029/2001JD001315.

Strecker, M. R.; Alonso, R. N.; Bookhagen, B.; Carrapa, B.; Hilley, G. E.; Sobel, E. R.; and Trauth, M. H. 2007. Tectonics and climate of the southern central Andes. Annu. Rev. Earth Planet. Sci. 35:747–787, doi:10.1146/annurev.earth.35.031306.140158.

Tassara, A.; Swain, C.; Hackney, R.; and Kirby, J. 2007. Elastic thickness structure of South America estimated using wavelets and satellite-derived gravity data. Earth Planet. Sci. Lett. 253:17–16, doi:10.1016/j.epsl.2006.10.008.

Tucker, G. E., and Slingerland, R. 1997. Drainage basin responses to climate change. Water Resour. Res. 33: 2031–2047.

Uba, C. E.; Strecker, M.; and Schmitt, A. K. 2007. Increased sediment accumulation rates and climate forcing in the central Andes during the late Miocene. Geology 35:979–982, doi:10.1130/G224025A.1.

Vernon, A. J.; van der Beek, P.; and Sinclair, H. D. 2009. Spatial correlation between long-term exhumation rates and present-day parameters in the western European Alps. Geology 37:859–862.

Watts, A. B.; Lamb, S. H.; Fairhead, J. F.; and Dewey, J. F. 1995. Lithospheric flexure and bending of the central Andes. Earth Planet. Sci. Lett. 134:9–21.

Whipple, K. X. 2004. Bedrock rivers and the geomorphology of active orogens. Annu. Rev. Earth Planet. Sci. 32: 151–185, doi:10.1146/annurev.earth.32.101802.120356.

———. 2009. The influence of climate on the tectonic evolution of mountain belts. Nature Geosci. 2:97–104, doi:10.1038/NGEO413.

Wittmann, H.; von Blanckenburg, F.; Guyot, J. L.; Maurice, L.; and Kubik, P. W. 2009. From source to sink: preserving the cosmogenic ^{10}Be-derived denudation rate signal of the Bolivian Andes in sediment of the Beni and Mamoré foreland basins. Earth Planet Sci. Lett. 288:463–474.

Wobus, C.; Whipple, K. X.; Kirby, E.; Snyder, N.; Johnson, J.; Spyropolou, K.; Crosby, B. T.; and Sheehan, D. 2006. Tectonics from topography: procedures, promise, and pitfalls. *In* Willett, S. D.; Hovius, N.; Brandon, M. T.; and Fischer, D., eds. Tectonics, climate and landscape evolution. Geol. Soc. Am. Spec. Pap. 398:55–74.

Zaprowski, B.; Pazzaglia, F. J.; and Evenson, E. B. 2005. Influences on profile concavity and river incision. J. Geophys. Res. 110:F03004, doi:10.1029/2004JF000138.

Zeilinger, G., and Schlunegger, F. 2007. Possible flexural accommodation on the eastern edge of the Altiplano in relation to focused erosion in the Rio La Paz drainage system. Terra Nova 19:373–380.